

An ab Initio Study of S_N2 Reactivity at C6 in Hexopyranose Derivatives. II. Role of Populations, Barriers, and Reaction Path Curvature

Richard Dawes, Kathleen M. Gough,* and Philip G. Hultin*

Department of Chemistry, University of Manitoba, Winnipeg, Manitoba R3T 2N2, Canada

Received: October 30, 2003; In Final Form: August 4, 2004

This paper continues our investigation into a simple dipole–dipole interaction model proposed to explain the dramatically reduced S_N2 reactivity at the primary C6 position of galacto-configured pyranose systems relative to their gluco isomers. We present ab initio calculations (B3LYP/6-31+G(d,p)) on six model structures that show that this effect is not a major influence. Reactant rotameric equilibria as well as free-energy reaction barriers and reaction path curvature were evaluated. Results point to a number of other factors that could account for the observed reactivity differences. Our results cast doubt on the general relevance of transition structure dipole–dipole repulsions to S_N2 reactivity.

Introduction

We have been investigating the anomalously low S_N2 reactivity toward anionic nucleophiles at the C6 position of hexopyranosides having the galacto configuration (i.e., C4–OR axial).¹ The corresponding gluco-configured compounds (C4–OR equatorial) react at rates typical of primary centers.² We are specifically interested in the electrostatic explanation that A. C. Richardson proposed in 1969.³ The details of his dipole–dipole interaction model are described in our previous paper.¹ The validity of this model has implications for the understanding of S_N2 reactivity in general. In the first paper of this series, we examined the magnitudes of dipole–dipole effects in these structures and found them insufficient to account for the observed differences in reactivity.

Despite the sluggishness of most S_N2 displacements at C6 in galactopyranose derivatives, there are examples in the literature of efficient reactions. The availability of potent leaving groups such as triflate has made some previously impractical transformations possible,⁴ but this technical improvement does not alter the intrinsic reactivity differences between gluco- and galacto-configurations. The situation is complicated by the fact that substrates having differing substituents remote from C6 often react at very different rates. For example, the tricyclic bis-(acetone) **a** reacted with azide by an order of magnitude more slowly than did the triacetate **b**,⁵ while the permethylated tosylate **c** reacted with NaI twice as fast as **a** (see Figure 1).⁶

Such observations are fundamentally inconsistent with a generalized transition-state dipole effect involving the C4–O fragment. First, this local dipole would not differ greatly among various 4-*O*-alkyl galactose derivatives. Second, electronegativity considerations suggest that the local C4–OAc dipole in more reactive **b** should be *greater* than the C4–OR dipole in the unreactive **a**. The changes in reactivity as other substituents are changed may arise from changes in pyranose ring conformations, or they may reflect differences in rotameric equilibria around the C5–C6 bond. That remote groups can influence C5–C6 rotation is clear from published studies on a series of alkyl

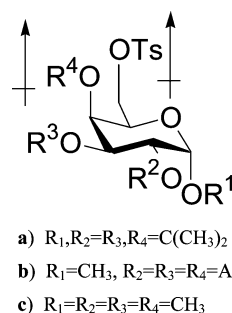


Figure 1. Examples of galacto-configured compounds with proposed dipole–dipole interactions illustrated.

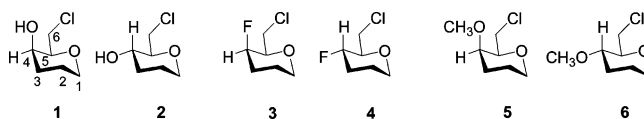


Figure 2. Tetrahydropyran model structures used in this study. Carbon atoms are designated using carbohydrate numbering.

galactopyranosides that showed that rotamer populations were significantly altered by changes in the aglycon structure.⁷

In this paper, we extend our ab initio study of S_N2 displacements in gluco- and galacto-configured model systems to include three different groups at the C4 position. We include the effects of solvation and reactant conformer populations in a kinetic analysis for all six systems. Our results indicate that neither steric nor dipolar effects can explain the observed reactivity differences in this class of S_N2 reactions. Our analysis casts doubt on the general validity of this popular rationalization, while revealing a number of important factors for displacements at primary positions in pyranosides.

Computational Models

We have expanded our study to include tetrahydropyran model structures 1–6 (Figure 2), again using chloride–chloride identity displacement reactions. In these models, hydrogens replace the C1, C2, and C3 hydroxyl groups of the monosaccharides, while the C4 hydroxyl is preserved or replaced by either fluorine or a methoxy group.

* Authors for correspondence. E-mail: hultin@cc.umanitoba.ca (P.G.H.); kmgough@ms.umanitoba.ca (K.M.G.).

Electronic structure calculations were performed using parallel-enabled *Gaussian 98*,^{8a} *Gaussian 98W*, and *Gaussian 03*.^{8b} Given the size of the model systems, and the number of electrons and degrees of freedom, the most reliable, yet affordable, level of theory was sought. Hybrid DFT methods have been used extensively and were validated for S_N2 reactions involving chloride by Parthiban et al. in 2001.⁹ A more recent study by Li et al.¹⁰ found good agreement between dynamics calculated with B3LYP and those observed experimentally. The systems considered by Li were CFCs that share the same atom types and fragment orientations studied here. All our calculations were therefore performed using the B3LYP/6-31+G(d,p) level of theory.

Searches for relevant reactant and transition structure geometries were undertaken. Stationary points were characterized through vibrational analysis. Initially, the C5–C6 rotamers of substrates **1–6**, including possible intramolecularly hydrogen-bonded species, were identified in a series of geometry optimizations. For **1**, **2**, **5**, and **6**, the possibility of permutations of hydroxyl or methoxy rotamers at C4 was also explored. Transition structures connecting the rotational minima were obtained. Beginning from these rotational minima, possible reaction coordinates for S_N2 displacements were located. From the S_N2 transition structures, the intrinsic reaction coordinates (IRCs) were obtained, and the free energy was maximized along these paths. These paths and free-energy maxima were obtained using the IRC and IRCMAX routines in *Gaussian 03*. The IRCMAX routine also calculated the curvature of the reaction coordinate at the free-energy maximum.

Corrections for basis set superposition errors (BSSEs) were calculated using the full counterpoise method of Boys and Bernardi.¹¹ These corrections were applied at the transition structure geometries using the “Counterpoise” keyword in *Gaussian 03*. Because these displacement reactions are typically carried out in DMF solvent, at elevated temperature, the effects of solvation and temperature on the calculated energy profiles were estimated. Two solvation models were used at the B3LYP/6-31+G(d,p) level. All of the structures and frequencies were recalculated with the Onsager dipole continuum model and a dielectric constant of 36.71 (chosen for DMF at 298 K). The geometries so obtained were then used to calculate solvated energies using the isodensity polarized continuum (IPCM) model.¹² The vibrations calculated under the Onsager solvation model were retained to provide free-energy corrections to the IPCM energies.

Boltzmann statistics were applied to the relative free energies to obtain rotameric populations. The thermal contributions to Gibbs free energies were calculated at each of three temperatures. Room temperature was included to allow comparison with other published results, while 373 and 413 K were chosen to represent realistic reaction conditions. Relative rates of S_N2 displacement (galacto/gluco) were calculated for each of the three pairs of systems.

With canonical variational transition state theory, reaction rates were calculated using the free-energy maxima along the IRC. The reaction path curvature was calculated at the free-energy maximum along the IRC.

Results and Discussion

Our gas-phase calculations located three rotational minima for each compound, corresponding to the expected staggered conformations. The calculated dihedral angles and energies for these rotamers are summarized in Tables 1 and 2. In all of the galacto models, the most stable rotamer was **tg**, while the

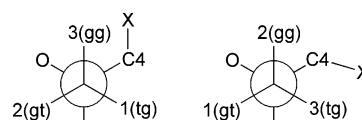


Figure 3. Newman projections along the C5–C6 bonds in **1–6**, showing possible positions for the chlorine atom, ranked as (1) preferred, (2) next, and (3) least preferred, for galacto (left) and gluco (right). (X = OH, F, OMe).

TABLE 1: Calculated Dihedral Angles ω ($^\circ$), Free Energies ΔG_{298}° (kcal mol $^{-1}$), and Percentage Populations for Exocyclic Chloromethyl Rotational Minima and Rotational Transition Structures of Galacto Structures **1, **3**, and **5****

structure	B3LYP/6-31+G(d,p)			B3LYP IPCM (DMF)		
	ω	ΔG_{298}°	% population	ω	ΔG_{298}°	% population
1gt	71.4	0.869	18.00	69.9	0.000	97.05
TS _{1gt-1tg}	116.8	3.414		120.8	5.223	
1tg	169.6	0.000	78.03	167.9	2.192	2.40
TS _{1tg-1gg-h}	243.7	5.108		241.6	6.724	
1gg-h	293.9	1.765	3.97	294.0	3.064	0.55
TS _{1gg-h-1gg}	300.8	6.148		NA	NA	
1gg	305.2	5.851	.004	NA	NA	NA
TS _{1gg-1gt}	354.4	9.150		353.4	9.352	
3gt	70.9	0.917	17.53	69.1	0.408	33.26
TS _{3gt-3tg}	116.1	3.349		117.5	3.971	
3tg	169.3	0.000	82.45	170.8	0.000	66.26
TS _{3tg-3gg}	248.8	8.315		246.5	6.473	
3gg	301.2	4.900	0.02	301.1	2.921	0.48
TS _{3gg-3gt}	355.5	8.901		356.4	7.803	
5gt	72.0	0.949	16.76	69.9	0.000	64.74
5tg	171.0	0.000	83.23	170.2	0.361	35.21
5gg	303.5	5.471	.008	305.3	4.225	0.05

TABLE 2: Calculated Dihedral Angles ω ($^\circ$), Free Energies ΔG_{298}° (kcal mol $^{-1}$), and Percentage Populations for Exocyclic Chloromethyl Rotational Minima and Rotational Transition Structures of Gluco Structures **2, **4**, and **6****

structure	B3LYP/6-31+G(d,p)			B3LYP IPCM (DMF)		
	ω	ΔG_{298}°	% population	ω	ΔG_{298}°	% population
2gt	72.1	0.000	77.09	71.4	0.000	48.36
TS _{2gt-2tg}	125.8	2.948		129.5	2.028	
2tg	147.6	1.568	5.46	147.2	0.239	32.30
TS _{2tg-2gg}	223.1	7.683		223.0	7.792	
2gg	295.7	0.880	17.44	295.9	0.543	19.35
TS _{2gg-2gt}	359.8	7.437		360.2	6.160	
4gt	71.0	0.000	60.66	72.0	0.000	52.39
TS _{4gt-4tg}	128.2	3.420		127.1	2.860	
4tg	157.6	2.085	1.80	158.0	1.281	6.03
TS _{4tg-4gg}	225.9	6.351		227.0	6.078	
4gg	295.0	0.284	37.54	294.4	0.137	41.58
TS _{4gg-4gt}	360.6	7.180		360.2	6.379	
6gt	70.2	0.000	51.69	70.0	0.000	68.71
6tg	142.7	2.391	0.91	NA	NA	NA
6gg	293.1	0.051	47.39	294.3	0.466	31.29

highest-energy rotamer was **gg**. In the gluco structures, the preferred conformation was always **gt**, while the least stable rotamer was **tg** (Figure 3).

A search of structures **1** and **2** for low-energy hydroxyl rotamers at C4 produced an additional minimum (**1gg-h**) in which the OH group was rotated to form a hydrogen bond with the Cl. The hydrogen-bonded conformation **1gg-h** was considerably more stable than **1gg**, but was still much higher in free energy than the **1tg** or **1gt** rotamers. A similar search of **5** and **6** for methoxy rotamers at C4 produced no additional low-energy structures. For each C6 rotamer, the methoxy group always preferred a position trans to the C4–C5 bond. Proper convergence to minima for the methoxy structures was problematic. The rotational potentials for the methoxy group at C4 are quite

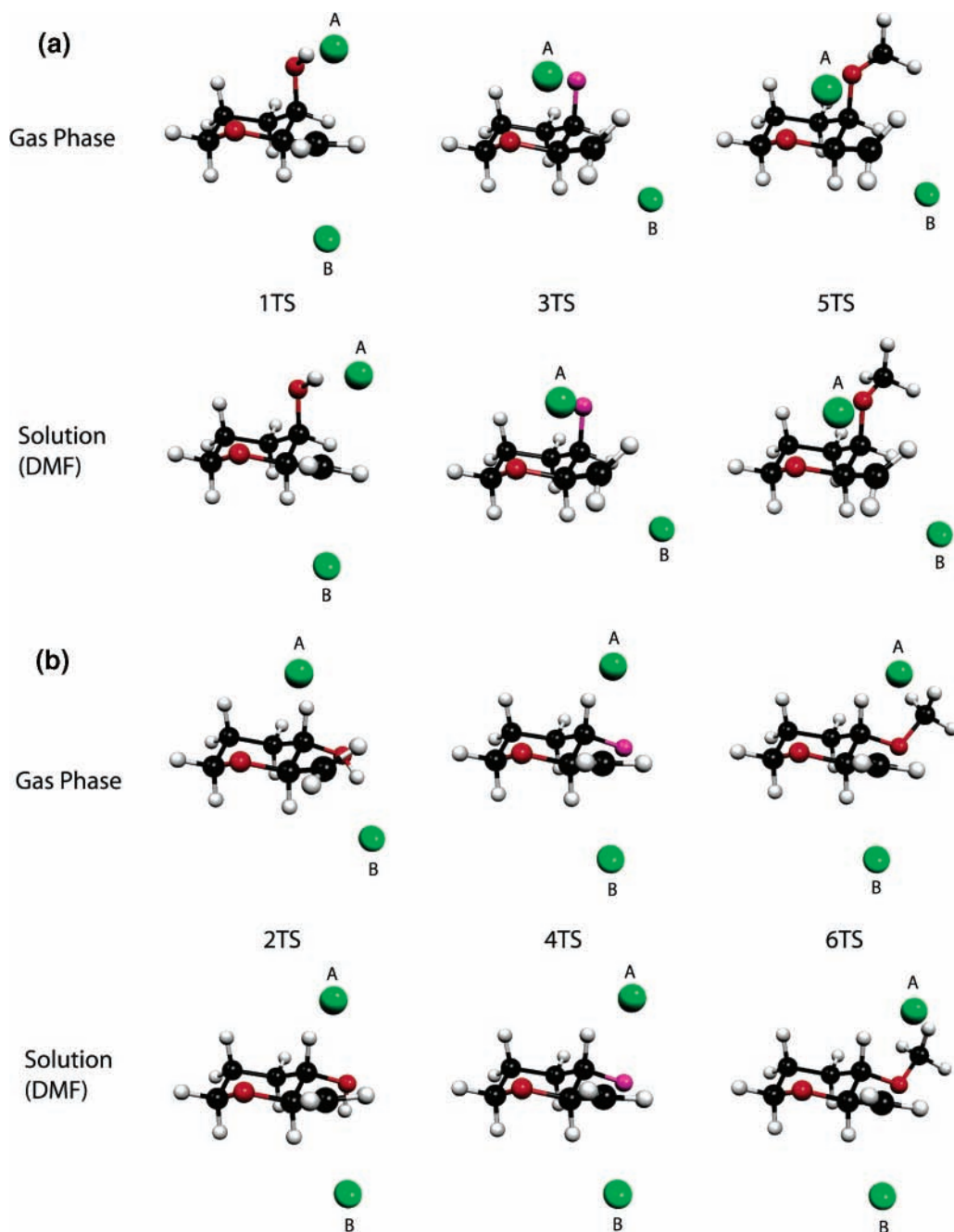


Figure 4. (a) Transition structures for identity S_N2 displacements of galacto compounds **1**, **3**, and **5** in the gas phase and with solvation. Chlorine atoms are labeled A and B for discussion purposes. (b) Transition structures for identity S_N2 displacements of gluco compounds **2**, **4**, and **6** in the gas phase and with solvation. Chlorines are labeled as in part a.

shallow near the global minimum, in some cases necessitating the recalculation of force constants at every point.

We located the rotational transition structures between the rotamers in **1–4**. These are included in Tables 1 and 2. Because of the convergence problems with **5** and **6**, and their otherwise typical rotamer energies, they were excluded from this analysis. In all cases, the rotational barriers were sufficiently low that the model systems would be in thermal equilibrium at the temperatures under consideration.

Calculations incorporating solvation by DMF (Onsager and IPCM) produced significant changes in the relative rotamer free energies for **1–6**. In the axial (galacto) cases **1**, **3**, and **5**, **gt** was stabilized considerably at the expense of **tg**, while **gg** remained a minor constituent. For the fluoro and methoxy systems, **gt** actually became the preferred rotamer. After optimization with the Onsager model, the hydrogen-bonded

geometry **1gg-h** was still a minimum. After the IPCM energy correction, the Onsager transition structure connecting **1gg** with **1gg-h** fell below **1gg**. Because **1gg** was no longer a stationary point, it was discarded from the set of reactive conformers.

In the equatorial (gluco) cases **2**, **4**, and **6**, solvation affected the **tg** rotamers differently in each system. The hydroxy model **2tg** was strongly stabilized, while the fluoro model **4tg** was only slightly stabilized. The already disfavored methoxy compound **6tg** (<1% of the population in the gas phase) was no longer a minimum on the rotational surface. Of all the **tg** rotamers, **6tg** is notable for having the smallest dihedral angle ω , nearly eclipsing the hydrogen at C5. With Onsager solvation, optimizations beginning at **6tg** converged to the **6gt** conformation. The **gg** rotamers were affected to a lesser extent by solvation and remained well populated (>19%) in all cases.

Our calculations reproduced the spread and qualitative

orderings of rotamer energies for both the galacto and gluco cases. Our rotamer populations and the barriers to their interconversion are in general accord with several recent experimental and theoretical studies of C5–C6 rotamer populations in D-glucopyranose and D-galactopyranose.⁷ The population trend in galactose derivatives typically is $P_{\text{tg}} \approx P_{\text{gt}} > P_{\text{gg}}$. The energy differences between **gg** and **tg/gt** rotamers have been found to be quite large, and the population of the **gg** rotamer depends strongly on substituent and solvent effects. In contrast, glucose derivatives generally display a narrower range of rotamer energies, with relative populations $P_{\text{gg}} > P_{\text{gt}} > P_{\text{tg}}$ in most cases. Significantly, in gluco-configured compounds, the **gg** rotamer remains well-populated as substituent groups on other positions are changed and as solvents are varied. Our calculated populations for gluco model **4** are within 3% of those calculated by Hoffmann and Rychlewski for 4-deoxy-4-fluoro-D-glucopyranose, once their further subdivided results are summed into the three C5–C6 rotamer categories.¹³ We also note that a recent NMR study of 6-deoxy-6-iodo-D-glucose in D₂O solution showed that the **gg** and **gt** rotamers were both well-populated.^{7a} These results suggest that our model systems are indeed appropriate for the hexopyranoses under evaluation.

S_N2 Transition Structures. Transition structures for the S_N2 displacements were sought beginning from each of the rotational minima of the new systems. As in our previous study,¹ in each model system, only one S_N2 transition structure was found (see Figure 4a b). For the galacto compounds, these transition structures connect the **gg** and **tg** rotamers. For the gluco compounds, the transition structures connect the **gg** and **gt** rotamers. Because these are identity reactions, they could proceed in either direction. For discussion purposes, we have labeled the chlorine “above” the plane of the ring as Cl_A and the other as Cl_B. To facilitate structural comparison with the reactant rotamers, we identify the O5–C5–C6–Cl torsion angles as ω_A and ω_B for Cl_A and Cl_B, respectively.

According to the dipole–dipole repulsion model, the Cl_A–C6–Cl_B group would be expected to be oriented perpendicularly to the ring system, to avoid repulsive interactions with the ring oxygen, although this would create a repulsive interaction with the galacto substituent at C4, destabilizing the **TS**. At first glance, it may appear that galacto compounds **3TS** and **5TS** are twisted to avoid a repulsive interaction at C4, while compound **1TS** is only prevented from twisting by a hydrogen bond. Interestingly, however, with solvation and the consequent decrease in the importance of the hydrogen bond in **1TS**, ω_A actually decreases, with Cl_A relaxing further from O5 just as in the other cases. The relaxation of the H-bond (gas phase: $r_{\text{H-Cl}} = 2.066 \text{ \AA}$; $\theta_{\text{O-H-Cl}} = 5.5^\circ$. solvated: $r_{\text{H-Cl}} = 2.128 \text{ \AA}$; $\theta_{\text{O-H-Cl}} = 18.0^\circ$) occurs through a torsional motion of the hydroxyl at C4. The S_N2 transition structures for reactions of the galacto structures **3** (fluoro) and **5** (methoxy) do have torsion angles ω_A inclined considerably toward O5, and solvation also produced a slight relaxation away from O5.

The Cl_A–C6–Cl_B deflection angles are approximately 150° in all systems; there is no exaggeration of this angle in the galacto compounds. We note that these angles are typical of calculated transition structures for S_N2 identity reactions involving chloride.¹⁴ As discussed in the first paper of this series,¹ the classical dipole–dipole interaction energy is insufficient to explain the energy difference between the gluco and galacto systems, even for perfectly aligned dipoles. Because of the ~150° deflection angle, this interaction would be further reduced, and insufficient to drive the torsion toward O5. We

therefore do not attribute the torsion angles in **3TS** and **5TS** to repulsive dipolar interactions.

This conformational preference in the transition structures can be correlated with the energies and rotational potentials of the reactant rotamers (see Table 1). The orientation of the Cl_A–C6–Cl_B group shows a strong dependence on the reactant C5–C6 rotational potentials in both the galacto and gluco systems. One chlorine (denoted here as Cl_A) must always occupy a position analogous to the **gg** rotamer and is not a determining factor in either the galacto or gluco systems. In **1**, the preferred rotamer is **1gt** by a significant margin, and the **1TS** torsion angle reflects this. In **3TS** and **5TS**, ω_B is within 15° of that found in the preferred rotamers **3tg** and **5tg**. In the gluco cases, the **tg** rotamer becomes increasingly disfavored through the systems **2**, **4**, and **6** (see Table 2). Correspondingly, ω_B decreases through the transition structures **2TS**, **4TS**, and **6TS** (seen in Figure 4b) as the Cl_A–C6–Cl_B group twists increasingly toward the favored **gt** reactant rotamer orientations.

Factors Controlling Relative Rates. The reaction kinetics were modeled at two realistic temperatures (373 and 413 K) with the consideration of rotamer populations, reaction barriers, free-energy barriers, and reaction path curvature. The rates of reactions involving rapid pre-equilibria are generally interpreted in terms of Curtin–Hammett/Winstein–Holness kinetics. The rates of conversion between the C5–C6 rotamers of **1–6** corresponding to our calculated barriers are much greater than the rates of S_N2 displacement. In such a situation, the Curtin–Hammett Principle has sometimes been interpreted to mean that the outcome of the overall process is wholly independent of the equilibrium populations, depending only on the relative rate constants for the subsequent reaction. However, this is erroneous, as Seeman pointed out in his comprehensive 1983 review:¹⁵ “the ground state conformational preference has a direct (proportional) role” in the final product ratios. The relative rates of rotamer interconversion and S_N2 reaction derived from our calculations correspond to the “Scheme 2” kinetics of the Curtin–Hammett/Winstein–Holness analysis. The net rate constant for a reaction given these conditions can correctly be expressed as a mole-fraction-weighted sum of individual rate constants.¹⁶

As these are identity reactions, microscopic reversibility dictates that we consider a nucleophilic approach to both of the rotamers connected through the IRC. Thus, the total reaction rate is the sum of two equal contributions. Because the rotational barriers are much lower than the S_N2 barriers, the populations of reactive rotamers are constantly maintained. However, the total reactive population at any time is only the sum of the two reactive rotamers for each system. When comparing the total reaction rates between systems, the population of the third rotamer that does not directly participate in the reaction becomes important.

The relative rate of S_N2 displacement (galacto/gluco) can be written as the ratio of two sums, the mole-fraction-weighted rates for each system. This formulation is equivalent to more conventional expressions in terms of ensemble average free energies.¹⁵ We prefer eq 1 because it provides insight into the contributions of both the reactant states and the transition state to the overall barrier to the S_N2 reaction.

Relative rate galacto/gluco =

$$\frac{p_{\text{Galgg}}(T) \cdot \exp(-\Delta G_{\text{Galgg}}^\ddagger/RT) + p_{\text{Galtg}}(T) \cdot \exp(-\Delta G_{\text{Galtg}}^\ddagger/RT)}{p_{\text{Glugg}}(T) \cdot \exp(-\Delta G_{\text{Glugg}}^\ddagger/RT) + p_{\text{Glugt}}(T) \cdot \exp(-\Delta G_{\text{Glugt}}^\ddagger/RT)} \quad (1)$$

TABLE 3: Mole Fractions of Reactive Rotamers, Activation Free Energies ΔG^\ddagger (kcal mol⁻¹), Curvature, and Reaction Rates in S_N2 Identity Displacement Reactions of **1 through **6** with Cl⁻ Ion**

structure	<i>T</i> (K)	mole-fraction of rotamer	ΔG^\ddagger TS ^a	sum of reactive mole-fractions	curvature ^b of IRC (au)	net relative S _N 2 rate galacto/gluco				
1gg	373.15	0.0133	27.80	0.0631	1.08	0.020				
1tg		0.0498	28.78							
2gg		0.1987	26.92							
2gt	373.15	0.4596	27.54	0.6387	513.94	0.062				
3gg		0.0119	29.76							
3tg		0.6268	32.67							
4gg		0.3977	30.27							
4gt		0.5067	30.45							
5gg		0.0020	26.94							
5tg	373.15	0.3895	30.27	0.3915	505.75	0.061				
6gg		0.3319	28.64							
6gt		0.6681	29.16							
1gg		413.15	0.0185				28.76	0.0838	1.08	0.031
1tg			0.0653				29.80			
2gg			0.2005				27.88			
2gt	413.15	0.4507	28.54	.6283	513.94	0.084				
3gg		0.0169	30.62							
3tg		0.6114	33.57							
4gg		0.3889	31.17							
4gt		0.4975	31.37							
5gg		0.0034	27.86							
5tg	413.15	0.4039	31.17	0.4073	505.75	0.083				
6gg		0.3394	29.59							
6gt		0.6606	30.14							

^a Includes BSSE corrections. ^b Effect of curvature not included in rate constant.

In Table 3, the relative rates of S_N2 displacements for each of the three model systems are compared at two temperatures. The barriers are expressed in kilocalories per mole from the reactive rotamers. The barriers include the corrections for BSSE, which were approximately 0.30 kcal mol⁻¹ in all systems. As seen in Table 3, for hydroxy structures **1** and **2**, the barriers to reaction from the reactive rotamers are slightly higher for the galacto system. However, while the barriers do contribute to the low net relative rate in this case, the larger effect arises from the rotamer populations. The gluco system has a roughly 10-fold larger population of reactive rotamers. Considering systems **3–6** (fluoro and methoxy), we see that the barriers to the S_N2 reaction from the **gg** rotamers are actually lower for the galacto cases. However, this rotamer is not well-populated, never exceeding 2%, even at 413 K. The calculated S_N2 activation barriers from the more populated **tg** rotamers are considerably higher. The summed reactive populations are somewhat lower for the galacto cases, and the 5 kcal mol⁻¹ spread of rotamer energies means that the more populated rotamers have a larger barrier to overcome. In contrast, the gluco model rotamers were all within about 2 kcal mol⁻¹ of one another. The reactive conformer populations ranged from 65% to 100% in the three model systems at 413 K. These population differences would result in a dramatic lowering of reaction rates in the galacto compounds relative to their gluco counterparts (Table 3, last column) at either temperature.

As expected for S_N2 displacement reactions, the maxima in free energy along the IRC corresponded closely to the transition structures found from electronic energies. The furthest that any generalized transition state was found from the transition structure was 0.0045 amu^{1/2}·bohr for system **5**. The free energies at these points were identical (within reported accuracy) to the conventional transition structure energies. However, it was determined that the reaction paths for galacto compounds **3** and **5** include massive curvature near the transition state (Table 3).¹⁷ Reaction path curvature could account for a 2-fold decrease in rate¹⁸ for galacto systems **3** and **5**, and it has been suggested

that curvature can account for much larger rate reductions than this.¹⁹ Because of the size of these model systems, it was not possible for us to explore the effects of reaction path curvature quantitatively. The structural origin of such high curvature in these systems is an interesting question for future research.

It may seem unfortunate that Richardson's intuitive dipolar repulsion explanation must be discarded. However, the transition structure dipole model was essentially a yes/no argument. It implied that chemists should not even attempt reactions with certain substrates that may actually be feasible. The highlighted role of rotameric equilibria suggests that changing reaction conditions or substituents to alter these populations favorably may enhance reaction rates. Clearly, this could be accomplished in many ways, including destabilization of the normally dominant conformers. Experimental determination of rotamer populations using recently improved NMR methods will continue to provide insight into these factors.^{7a–c,20}

The dipole model was also proposed to explain stereochemically dependent reactivity differences in displacement reactions at secondary centers. In these situations, there is much less conformational mobility, and the putative interacting dipoles are much closer together. In these circumstances, dipole repulsion arguments may be more valid.²¹ We will be examining reactions of these types in future work.

Conclusions

Our results show that dipole–dipole interactions in the transition structures do not determine the relative reactivities in the model S_N2 reactions that we have studied. We find instead that the observed differences in S_N2 reaction rates probably can be attributed to a combination of factors including reactant rotamer populations, relative barriers, and reaction path curvature. Our results also suggest a significant contribution from reaction path curvature, but at present, it seems difficult to predict a priori how different substituents will influence this factor.

Acknowledgment. This work was funded by Natural Sciences and Engineering Council of Canada Research Grants to K.M.G. and P.G.H. Richard Dawes received a scholarship from Medicare, Inc. We thank Dr. Richard Bader and Mr. Chérif Matta (McMaster University), Dr. Tom Ziegler (University of Calgary), and Dr. Bob Wallace (University of Manitoba) for helpful discussions. The authors acknowledge the use of the University of Manitoba High Performance Computing Facilities (<http://www.umanitoba.ca/campus/acn/hpc/>). P.G.H. also thanks Dr. Walter A. Szarek (Queen's University) for suggesting the steric/dipole model to explain an unexpected result many years ago.

Supporting Information Available: Coordinates and absolute energies for all stationary points. This material is available free of charge via the Internet at <http://pubs.acs.org>.

References and Notes

- (1) Dawes, R.; Gough, K. M.; Hultin, P. G. *J. Phys. Chem. A* **2005**, *109*, 213.
- (2) Ball, D. H.; Parrish, F. W. *Adv. Carbohydr. Chem. Biochem.* **1969**, *24*, 139–197.
- (3) Richardson, A. C. *Carbohydr. Res.* **1969**, *10*, 395–402.
- (4) (a) Mulard, L. A.; Kovác, P.; Glaudemans, C. P. J. *Carbohydr. Res.* **1994**, *259*, 117–119. (b) Ali, M. A.; Hough, L.; Richardson, A. C. *Carbohydr. Res.* **1991**, *216*, 271–287.
- (5) Wu, M.-C.; Anderson, L.; Slife, C. W.; Jensen, L. J. *J. Org. Chem.* **1974**, *39*, 3014–3020.
- (6) Nadkarni, S.; Williams, N. R. *J. Chem. Soc.* **1965**, 3496.
- (7) (a) Brochier-Salon, M.-C.; Morin, C. *Magn. Reson. Chem.* **2000**, *38*, 1041–1042. (b) Rockwell, G. D.; Grindley, T. B. *J. Am. Chem. Soc.* **1998**, *120*, 10953–10963. (c) Padrón, J. I.; Morales, E. Q.; Vázquez, J. T. *J. Org. Chem.* **1998**, *63*, 8247–8258. (d) Morales, E. Q.; Padrón, J. I.; Trujillo, M.; Vázquez, J. T. *J. Org. Chem.* **1995**, *60*, 2537–2548. (e) Gregurick, S. K.; Kafafi, S. A. *J. Carbohydr. Chem.* **1999**, *18*, 867–890. (f) Lubineau, A.; Scherrmann, M.-C.; Mentech, J. Eur. Pat. Appl. EP 0 587 471 A1; *Chem. Abs.* **121**, 158095. (g) Zuccarello, F.; Buemi, G. *Carbohydr. Res.* **1995**, *273*, 129–145. (h) Brown, J. W.; Wladkowski, B. D. *J. Am. Chem. Soc.* **1996**, *118*, 1190–1193. (i) Wladkowski, B. D.; Chenoweth, S. A.; Jones, K. E.; Brown, J. W. *J. Phys. Chem.* **1998**, *102*, 5086–5092.
- (8) (a) Frisch, M. J.; Trucks, G. W.; Schlegel, H. B.; Scuseria, G. E.; Robb, M. A.; Cheeseman, J. R.; Zakrzewski, V. G.; Montgomery, J. A.; Stratmann, R. E.; Burant, J. C.; Dapprich, S.; Millam, J. M.; Daniels, A. D.; Kudin, K. N.; Strain, M. C.; Farkas, O.; Tomasi, J.; Barone, V.; Cossi, M.; Cammi, R.; Mennucci, B.; Pomelli, C.; Adamo, C.; Clifford, S.; Ochterski, J.; Petersson, G. A.; Ayala, P. Y.; Cui, Q.; Morokuma, K.; Malick, D. K.; Rabuck, A. D.; Raghavachari, K.; Foresman, J. B.; Cioslowski, J.; Ortiz, J. V.; Stefanov, B. B.; Liu, G.; Liashenko, A.; Piskorz, P.; Komaromi, I.; Gomperts, R.; Martin, R. L.; Fox, D. J.; Keith, T.; Al-Laham, M. A.; Peng, C. Y.; Nanayakkara, A.; Gonzalez, C.; Challacombe, M.; Gill, P. M. W.; Johnson, B. G.; Chen, W.; Wong, M. W.; Andres, J. L.; Head-Gordon, M.; Replogle, E. S.; Pople, J. A. *Gaussian 98W*, revision A.7 or A.11parallel; Gaussian, Inc.: Pittsburgh, PA, 1998. (b) Frisch, M. J.; Trucks, G. W.; Schlegel, H. B.; Scuseria, G. E.; Robb, M. A.; Cheeseman, J. R.; Montgomery, J. A., Jr.; Vreven, T.; Kudin, K. N.; Burant, J. C.; Millam, J. M.; Iyengar, S. S.; Tomasi, J.; Barone, V.; Mennucci, B.; Cossi, M.; Scalmani, G.; Rega, N.; Petersson, G. A.; Nakatsuji, H.; Hada, M.; Ehara, M.; Toyota, K.; Fukuda, R.; Hasegawa, J.; Ishida, M.; Nakajima, T.; Honda, Y.; Kitao, O.; Nakai, H.; Klene, M.; Li, X.; Knox, J. E.; Hratchian, H. P.; Cross, J. B.; Adamo, C.; Jaramillo, J.; Gomperts, R.; Stratmann, R. E.; Yazyev, O.; Austin, A. J.; Cammi, R.; Pomelli, C.; Ochterski, J. W.; Ayala, P. Y.; Morokuma, K.; Voth, G. A.; Salvador, P.; Dannenberg, J. J.; Zakrzewski, V. G.; Dapprich, S.; Daniels, A. D.; Strain, M. C.; Farkas, O.; Malick, D. K.; Rabuck, A. D.; Raghavachari, K.; Foresman, J. B.; Ortiz, J. V.; Cui, Q.; Baboul, A. G.; Clifford, S.; Cioslowski, J.; Stefanov, B. B.; Liu, G.; Liashenko, A.; Piskorz, P.; Komaromi, I.; Martin, R. L.; Fox, D. J.; Keith, T.; Al-Laham, M. A.; Peng, C. Y.; Nanayakkara, A.; Challacombe, M.; Gill, P. M. W.; Johnson, B.; Chen, W.; Wong, M. W.; Gonzalez, C.; Pople, J. A. *Gaussian 03*, revision A.1; Gaussian, Inc.: Pittsburgh, PA, 2003.
- (9) Parthiban, S.; Oliveira, G.; Martin, J. M. L. *J. Phys. Chem. A* **2001**, *105*, 895–904.
- (10) Li, B.; Liu, J.; Li, Z.; Wu, J.; Sun, C. *J. Chem. Phys.* **2004**, *13*, 6019–6027.
- (11) (a) van Duijneveldt, F. B.; van Duijneveldt-van de Rijdt, J. G. C. M.; van Lenthe, J. H. *Chem. Rev.* **1994**, *94*, 1873–1885. (b) Boys, S. F.; Bernardi, F. *Mol. Phys.* **1970**, *19*, 553–566.
- (12) Foresman, J. B.; Keith, T. A.; Wiberg, K. B.; Snoonian, J.; Frisch, M. J. *J. Phys. Chem.* **1996**, *100*, 16098–16104.
- (13) Hoffmann, M.; Rychlewski, J. *J. Am. Chem. Soc.* **2001**, *123*, 2308–2306.
- (14) Lee, I.; Kim, C. K.; Chung, D. S.; Lee, B.-S. *J. Org. Chem.* **1994**, *59*, 4490–4494.
- (15) Seeman, J. I. *Chem. Rev.* **1983**, *83*, 83–134.
- (16) See eq 20 in ref 15.
- (17) Miller, W. H.; Handy, N. C.; Adams, J. E. *J. Chem. Phys.* **1980**, *72*, 99.
- (18) Miller, W. H. *J. Chem. Phys.* **1982**, *76*, 4904.
- (19) Wang, H. W.; Hase, W. L. *Chem. Phys.* **1996**, *212*, 247.
- (20) Tvaroška, I.; Taravel, F. R.; Utille, J. P.; Carver, J. P. *Carbohydr. Res.* **2002**, *337*, 353–367.
- (21) Gronert, S.; Pratt, L. M.; Mogali, S. *J. Am. Chem. Soc.* **2001**, *123*, 3081–3091.